



St. Joseph's Journal of Humanities and Science

ISSN: 2347 - 5331

<http://sjctnc.edu.in/6107-2/>



CRYSTAL STRUCTURE, MORPHOLOGY, OPTICAL PROPERTY OF HYDROTHERMALLY SYNTHESIZED CdO@TiO₂ CORE-SHELL AND THEIR PHOTOCATALYTIC ACTIVITY

- A. Vijayabalan*

Abstract

The CdO@TiO₂ core-shell was prepared by hydrothermal method. XRD reveals that the shell as tetragonal body centered anatase TiO₂ and EDX confirms the core-shell. HR-SEM images show that the two or three particles fused together. Core-shell absorb is only in UV region but not in visible region. PL spectra show the strong blue emission. TiO₂ and core-shell both possess the same photocatalytic activity.

Keywords: Photoconductor, UV-A light, CdO, Titanium isopropoxide, CTAB, Rhodamine-B.

INTRODUCTION

Core-shell nanoparticles attract much attention because they have emerged at the frontier between materials chemistry and many other fields like biomedical, pharmaceutical, optical, electronics, and catalysis; Fig.1 displays, a typical core-shell nanoparticle. They are highly functional materials with modified properties. Sometimes properties arising from either core or shell materials can be quite different. The properties can be modified by changing the core to shell ratio itself. Because of the shell material coating, the properties of the core particle like reactivity and thermal stability can be changed. This may modify the overall particle stability and the dispersibility of the core particle. The purpose of the coating on the core particle are many fold, such as surface modification, the ability to increase the functionality, stability, and dispersibility, controlled release of the core, reduction in consumption of precious materials, and so on. Tuning

of such properties by surface modification enables the core-shell nanoparticles to be used in biomedical field, especially for bioimaging, controlled drug release, targeted drug delivery, cell labeling, and tissue engineering applications. In catalysis point of view, the main advantages of such particles are modified optical and electrical properties, chemical stability, morphology, etc. CdO is an n-type semiconductor with a direct band gap of 2.5 eV and an indirect band gap of 2.0 eV [1]. CdO nanostructures have low ohmic resistivity and high optical transmittance. The small band gap enables CdO to get photoexcited under visible light and act as photocatalyst. Phenols [2-4], naphthol [5] and organic dyes such as pyronine B and safranin T [6] are photodegraded by CdO. TiO₂ is an n-type semiconductor with direct bandgap 3.2 eV and indirect bandgap 3.0 eV. TiO₂ photocatalyst is widely used for mineralisation of organic contaminants. The charge- transfer resistance of Au@ZnS thin films gets reduced with an increase in concentration of Au core

*Assistant Professor, Department of Chemistry, St. Joseph's College of Arts and Science (Autonomous), Manjakuppam, Cuddalore, Tamil Nadu, India.
Cell: +91 9751061520, E-mail: vijayabalanchem@gmail.com

[7]. Reports on synthesis of core-shell nanoparticles are many [8] and Choudhuri and Paria[9] have recently listed the same. Semiconductor core-shell nanoparticles are being prepared by methods like precipitation, wet chemical reaction, precipitation in microemulsion, etc. Some of the core-shell nanoparticles prepared so far are $\text{Fe}_2\text{O}_3@\text{TiO}_2$, [10-14] $\text{Fe}_2\text{O}_3@\text{ZnO}$, [15,16] $\text{CeO}_2@\text{TiO}_2$, [8] etc. Literature search shows that $\text{CdO}@\text{TiO}_2$ and $\text{CdO}@\text{ZnO}$ core-shell nanoparticles have not been prepared so far. The conduction band of CdO core is less cathodic than those of TiO_2 and ZnO shells and the valence band hole is less anodic than those of TiO_2 and ZnO shells.



Fig. 1 : Core-Shell Nanoparticles

Ghows et al., reported that the CdS/TiO_2 nanoparticles have enhanced photocatalytic activity for RB_5 than pure TiO_2 and CdS under ultra sonication. The increased catalytic activity of nanocomposites in the presence of ultra sound is due to the enhancement of mass transfer, cleaning and sweeping the surface of catalyst and preventing the aggregation of particles [17]. Zhang *et al.* reported that the develop a rational synthesis strategy for the preparation of one-dimensional (1D) mesoporous $\text{Fe}_2\text{O}_3@\text{TiO}_2$ core-shell composites. In this strategy, FeO-OH nanorods are firstly coated by TiO_2 shell, followed by a calcination process, enhanced photocatalytic activity for the degradation of methyl orange under UV light irradiation and Rhodamine B under visible light irradiation [18]. Jiang et al. reported that the $\text{TCNQ}@\text{TiO}_2$ visible photocatalyst with core-shell structure was synthesized by adsorption methods; The photocatalyst activity of $\text{TCNQ}@\text{TiO}_2$ was enhanced gradually with the increasing proportion of TCNQ. The apparent rate constant k of $\text{TCNQ}@\text{TiO}_2$ -20% is 0.2583 h^{-1} , which is almost 67.9 times as high as that of pure TiO_2 . Under visible irradiation, the photogenerated holes on the HOMO orbit of TCNQ can be injected into the VB of TiO_2 , resulting in the oxidation of organic contamination [19]. MWCNT/ TiO_2 core-shell nanocomposites were obtained from a

newly developed coating approach The MWCNT/ TiO_2 core-shell nanocomposites exhibited conversion of CO_2 into methane in a continuous process under a low power visible light irradiation at atmospheric pressure [20]. Dong *et al.* (2015) reported that the prepared $\text{CdS}@\text{TiO}_2$ nanorods exhibit enhanced photocatalytic activities for phenol photodecomposition under visible light irradiation. The improved photoactivity is ascribed to the efficient separation of photogenerated electron and hole charge carriers between CdS cores and TiO_2 shells [21] In this paper, it is reported that the prepared $\text{CdO}@\text{TiO}_2$ core-shell and its characterization are used for degradation of rhodamine B under UV light.

MATERIALS AND METHODS

Materials

Titanium isopropoxide (Hi-media), Cadmium nitrate (Sd-fine), Cetyl trimethyl ammonium bromide (Hi-media), liquid ammonia (Qualigens), MacConkey agar (Hi-media) nutrient broth (SRL) and doubly distilled deionized water.

Synthesis of $\text{CdO}@\text{TiO}_2$ Core-Shell Particles

To an aqueous solution of $\text{Cd}(\text{NO}_3)_2$ (0.5 g in 25 mL) 1:1 aqueous ammonia was added to reach a pH of 9.5. The precipitated $\text{Cd}(\text{OH})_2$ was filtered, dried and calcined at 300°C for 30 min to get CdO nanoparticles. The synthesized cdo nanoparticles were suspended in distilled ethanol (0.1g in 10mL) under sonication for 10 min and 4.8 ml of titanium isopropoxide was added dropwise with stirring. This was followed by cetyl trimethyl ammonium bromide in ethanol (10 mL, 0.01 M), also under stirring in 1 h. The contents were transferred to a Teflon lined stainless steel autoclave vessel (100 mL), sealed and heated at 150°C for 14 h in an air oven. After allowing it to cool to room temperature, the crystals were collected by filtration, washed, dried and calcined at 500°C for 2 h in a muffle furnace fitted with a PID temperature controller.

RESULTS AND DISCUSSION

Crystal Structure

The X-ray diffraction pattern of $\text{CdO}@\text{TiO}_2$ core-shell particles synthesized by hydrothermal method using cetyl trimethyl ammonium bromide as modifying agent is presented in Fig.2 (a). It reveals the crystal structure

of the TiO₂ shell as tetragonal body centered anatase with lattice parameters *a* and *b* as 0.3777 nm and *c* as 0.9501 nm.

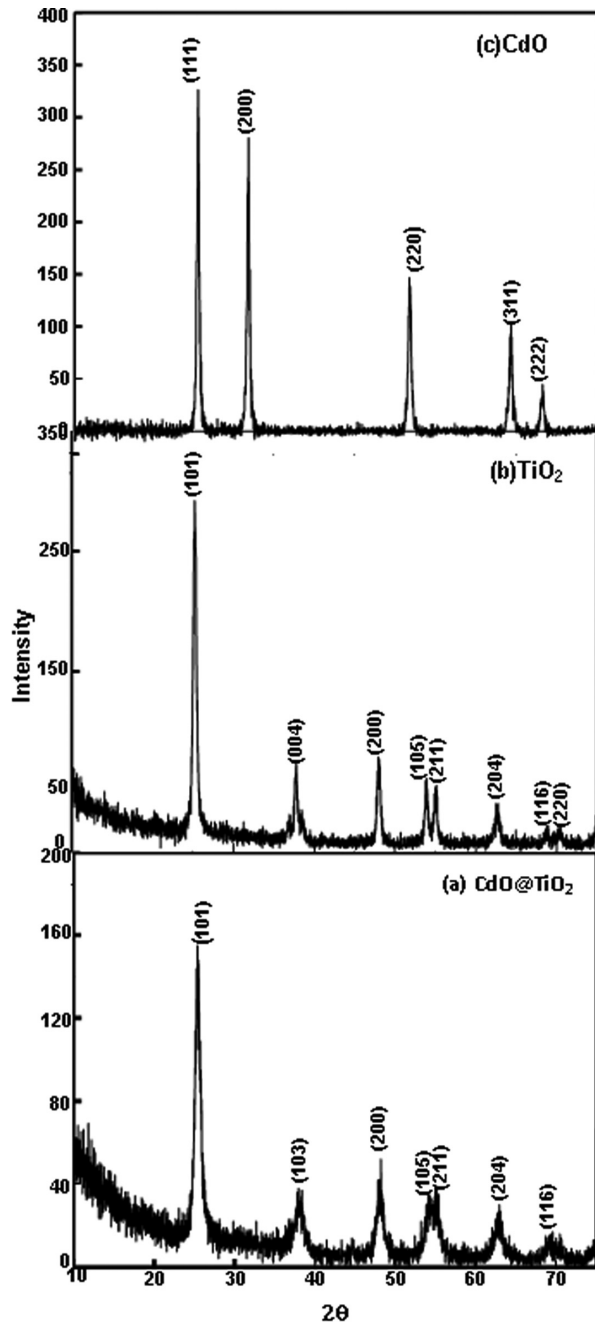


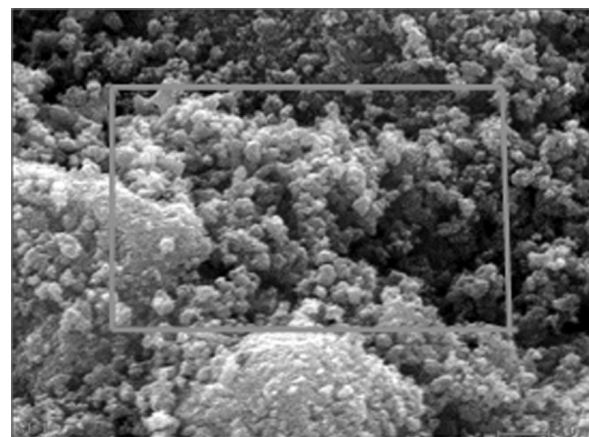
Fig.2 : Powder X-ray Diffraction Spectra

The XRD pattern matches totally with the standard JCPDS pattern of anatase (89-4921). The absence of rutile reflections (89-4920) shows the absence of rutile phase in the TiO₂ shell. The XRD of the precursor CdO, used to synthesize the core-shell particles, is shown in Fig.2(c). The displayed diffractogram matches with face centered cubic lattice of CdO (JCPDS no .65-2908), confirming the crystal structure of CdO core. The average crystallite size (*D*) of the synthesized

CdO has been obtained from the half-width of the full maximum (HWM) of the most intense peak using the scherrer equation $D = 0.9\lambda/\beta \cos \theta$, where *D* is the average crystallite size, λ is the wavelength of X-rays used, θ is the diffraction angle and β is the full width at half maximum of the peak. The average crystallite size of CdO is 57 nm. The X-ray diffractograms of TiO₂ following the reported procedures but in absence of CdO precursor shown in Fig.2 (b). The displayed XRD patterns show the prepared TiO₂ as anatase TiO₂. The XRD peaks match with those of JCPDS card no. 89-4921 revealing the tetragonal body centered lattice with unit cell lengths *a* and *b* as 0.3777 nm and *c* as 0.9501 nm. The average crystal sizes of TiO₂ are 34.

Analysis of Elemental Composition

The energy dispersive X-ray (EDX) spectra of CdO@TiO₂ core-shell particles are shown in Fig.3. It confirms the presence of TiO₂ shell in the prepared core-shell particles. They display the presence of Ti and the absence of Cd. The core CdO is deeply buried underneath the TiO₂ shell and the X-rays employed in the EDX analysis do not penetrate beyond the TiO₂ shell. It is well known that, X-rays penetrate only a few interplaner distances in crystals, which correspond to a couple of nanometers of the TiO₂ shell.



c:\edax32\genesis\genmaps.spc 27-Mar-2012 11:55:21
LSecs : 81

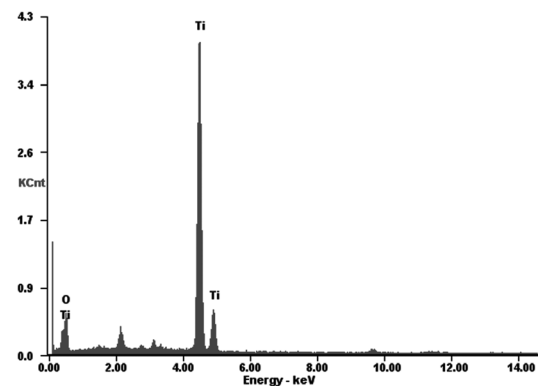


Fig.3 : EDX Spectrum of CdO@TiO₂ Core-Shell

Morphology

The High Resolution Scanning Electron Microscopic (HR-SEM) images of CdO@TiO₂ core-shell particles at different magnifications are displayed in Figs.4. It appears that most of the particles are made up of two or three spherically shaped particles fused together. The spherical shape of the constituent units is due to the use of CTAB.

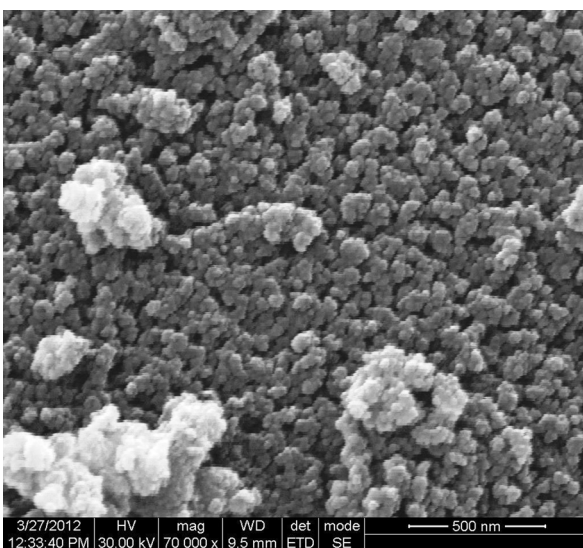
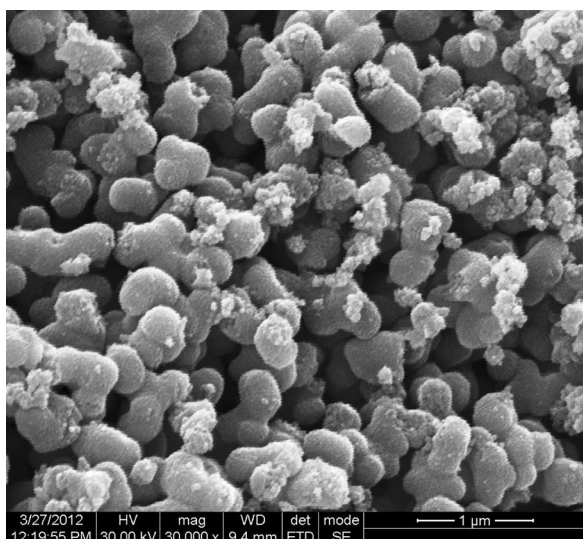


Fig.4 : HR-SEM Images of CdO@TiO₂

Optical Properties

The diffuse reflectance spectra (DRS) of CdO@TiO₂ core-shell particles are shown in Fig.5. The displayed DRS are in terms of $F(R)$, deduced by the application of Kubelka-Munk algorithm, $F(R) = (1 - R^2)/2R$, where R is the reflectance. The DRS of the core-shell particles

showed that they do not absorb visible light but absorb UV-A light. This confirms the TiO₂ shell in the prepared core-shell particles. Also, it could be inferred that the prepared materials are not CdO-TiO₂ composites; CdO absorbs visible light. The direct band gap of CdO@TiO₂ particles have been obtained through Tauc plots of $[F(R)hv]^2$ versus hv , as shown in Fig.6. Tauc plots of $[F(R)hv]^{0.5}$ versus photon energy, which provide the indirect band gaps of the core-shell oxides shown in the Fig.7. The deduced band gaps of CdO@TiO₂ are comparable with that of TiO₂ but not with that of precursor CdO. This confirms the perfect TiO₂ shell of the prepared core-shell particles. Figs.5, 6 and 7 also displays the direct and indirect band gap of precursor CdO, respectively.

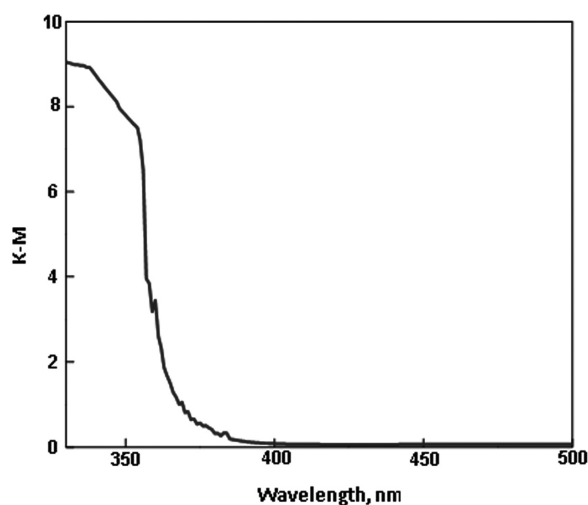


Fig.5 : DRS spectrum of Core-Shell

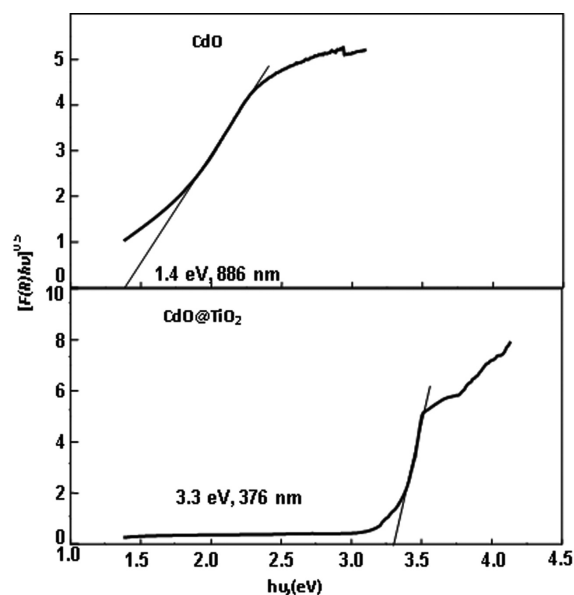


Fig.6 : Tauc Plot for Indirect Band Gap of Core-

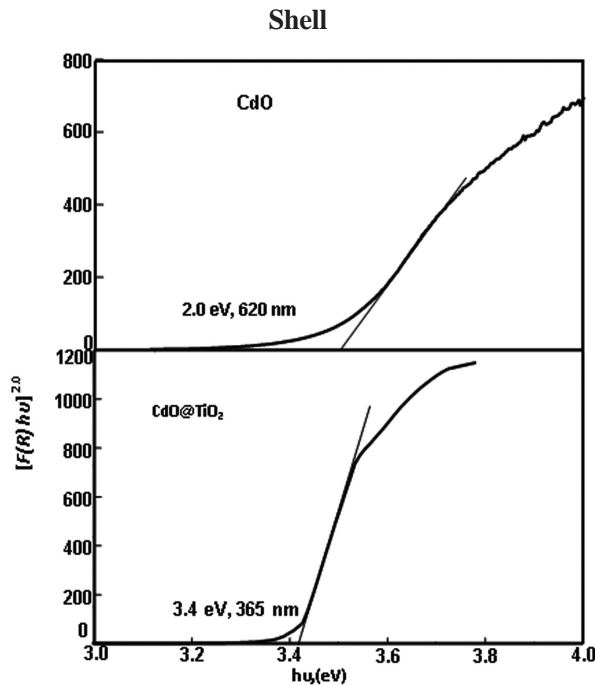


Fig.7 : Tauc Plot For Direct Band Gap of Core-Shell Photoluminescence

The photoluminescence (PL) spectra of CdO@TiO₂ core-shell particles are shown in Fig.8. The PL spectra of TiO₂ prepared by hydrothermal method, adopting the procedure followed for the synthesis of core-shell oxides but without using CdO. The emission spectrum of CdO@TiO₂ and bare TiO₂ both are similar. They show blue emission at 420 and 482 nm. These emissions are mainly because of crystal defects and the strong blue emission at 419 nm is likely due to oxygen vacancies in the lattice [16]. These results on the emission of CdO@TiO₂ and TiO₂ particles support the perfect TiO₂ shell in the CdO@TiO₂ core-shell particles.

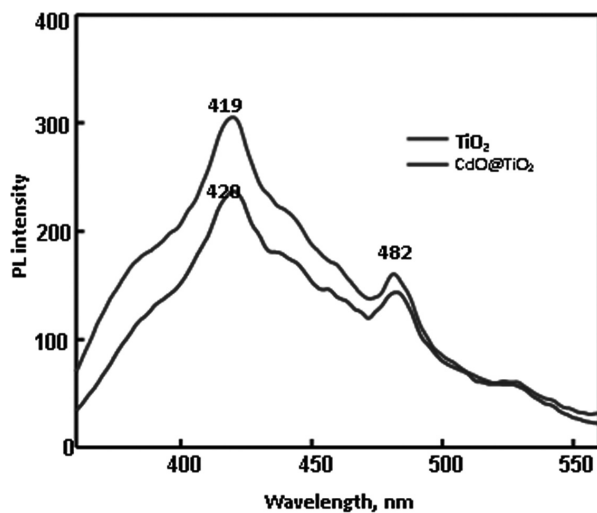


Fig.8 : PL Spectra

Photocatalytic Activity

The photocatalytic activities of CdO@TiO₂ particles have been tested with UV-A light using rhodamine B as model dye is shown in Fig.9. The results are corrected for adsorption. The profiles of dye degradation on pristine TiO₂ and CdO are also presented for comparison. The photocatalytic activity of CdO@TiO₂ and TiO₂ are similar; but CdO shows poor photocatalytic activity. The observed low photocatalytic activity of CdO is not surprising. In the photocatalytic oxidation of iodide ion also similar results are reported [17]. Photogeneration of electron-hole pairs, their recombination, interfacial charge transfer, light absorption efficiency, adsorption of water molecule, molecular oxygen and dye molecule, etc., determine the photocatalytic efficiency of a semiconductor. TiO₂ anatase is a more efficient photocatalyst than CdO. The conduction band (CB) electron in CdO is less cathodic than that of TiO₂ and also the valence band (VB) hole of CdO is less anodic than that of TiO₂. This is expected to decrease the photocatalytic activity. It is, the core-shell oxides are to be less photocatalytic active than pristine TiO₂. The photoexcited electron in the CB of TiO₂ in CdO@TiO₂ is expected to slip to the CB of CdO. Similarly, the photogenerated hole in the VB of TiO₂ in CdO@TiO₂ is expected to move to the VB of CdO.

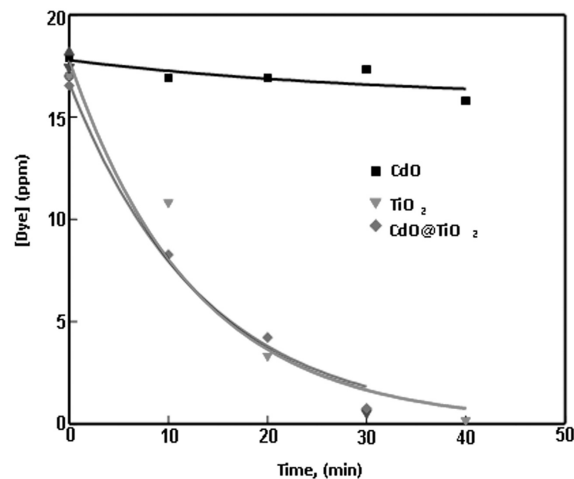


Fig.9: Degradation of rhodamine B under UV light

Absolute Vacuum Scale

The energy positions of the CB edges and VB edges of TiO₂ and CdO on the Absolute Vacuum Scale (AVS) are shown in the Fig.10. They determine the charge transfer from TiO₂ to CdO; the AVS is related to the normal hydrogen electrode (NHE) scale by $E_{(AVS)}$

$= -E_{(\text{NHE})} - 4.5$. The energy difference between the CB electrons of TiO_2 and CdO is the driving force for the interparticle electron injection and the free energy change is given by $-\Delta G = e[E_{\text{CB}(\text{CdO})} - E_{\text{CB}(\text{TiO}_2)}]$ [18-19]. Similarly, the energy difference between the VB holes of TiO_2 and CdO is responsible for the interparticle hole injection. This movement of photogenerated electron and hole from TiO_2 shell to CdO core should result in recombination of the photogenerated charge carriers in CdO core thus suppressing the photocatalytic activity. But such suppression of photocatalytic activity is not observed in the prepared CdO@TiO_2 core-shell oxides. An acceptable explanation is that the photogenerated charge carriers effectively take up the adsorbed water molecules or hydroxide ions or dye molecules and molecular oxygen resulting in photocatalysis.

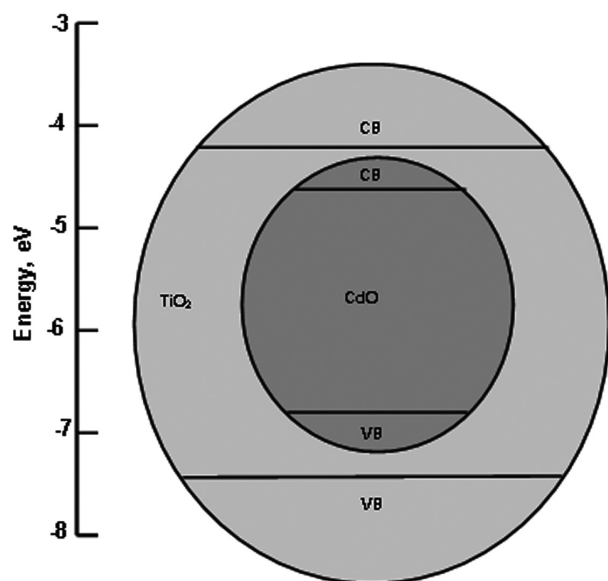


Fig.10 : Band Gap Energy Levels (AVS) of CdO@TiO_2

CONCLUSION

The CdO@TiO_2 core-shell was prepared by hydrothermal method. XRD pattern reveals that the tetragonal body centered anatase of TiO_2 shell and EDX confirms the core-shell. HR-SEM images show that the two or three particles fused together. Core-shell is only capable to absorb UV region but not visible region. PL spectra show the strong blue emission of the prepared sample. TiO_2 and core-shell both are having the same

photocatalytic activity efficiency.

REFERENCE

- De A. Reyes, M.E, Delgado, G.T, Perez, R.C, Marin, J.M, Angel, O.Z, (2012) Optimization of the photocatalytic activity of $\text{CdO} + \text{CdTiO}_3$ coupled oxide thin films obtained by sol-gel technique, *J. Photochem. Photobiol. A*, 228, 22-27.
- Karunakaran, C, Dhanalakshmi, R, (2008) Semiconductor-catalyzed degradation of phenol with sunlight, *Solar Energy Mater. Solar Cells*, 92, 1315-1321.
- Karunakaran, C, Dhanalakshmi, R, (2009) Selectivity in photocatalysis by particulate semiconductors, *Cent. Eur. J. Chem.* 7, 134-137.
- Karunakaran, C, Dhanalakshmi, R, Gomathisankar, P, Manikandan, G. (2010) Enhanced phenol-photodegradation by particulate semiconductor mixtures: Interparticle electron-jump, *J. Hazard. Mater.* 176, 799-806.
- Karunakaran, C, Narayanan, S, Gomathisankar, P, (2010) Photocatalytic degradation of 1-naphthol by oxide ceramics with added bacterial disinfection, *J. Hazard. Mater.* 181, 708-715.
- Li, J, Ni, Y, Liu, J, Hong, J, (2009) Preparation, conversion, and comparison of the photocatalytic property of $\text{Cd}(\text{OH})_2$, CdO , CdS and CdSe , *J. Phys. Chem. Solid.* 70, 1285-1289.
- Misra, M, Gupta, R.K, Single, M, (2015) Influence of gold core concentration on visible photocatalytic activity of gold-zinc sulfide core-shell nanoparticles; *J. Power Source*, 294, 580-587.
- Correa, D.N, De se Silva, J.M, Santos, E.B, Sigoli, F.A, Filho, A.G.S and Mazali, I.O, Study of Structure of the TiO_2 - MoO_3 bilayer films by raman spectroscopy (2011) *J. Phys. Chem. C*, 115, 10380.
- Choudhuri, R.G and Paria, S, (2012) *Chem. Rev.*, 112, 2373.
- Amal, R, Low, G and McEvoy, S, Novel photocatalyst titania coated magnetite, activity and photodissolution (2000) *J. Phys. Chem. B*, 104, 4387.
- Ao, Y, Xu, J, Fu, D, Shen, X and Yuan, C, magnetic semiconductor nanophotocatalysts for the

- degradation of organic pollutants (2008) Sep. Purif. Technol.61, 436.
12. Xuan, S.H, Jiang, W.Q, Gong, X.L, Hu, Y and Chen, Z.Y, fabrication and magnetic properties of hierarchial nickel microwires (2009) *J. Phys. Chem. C*, 113, 553.
 13. Xu, X and Cabuil, V, *J.nanometric core-shell gama-fe2o3/sio2/tio2 particles* (2009) *Nanopart. Res.*, 11, 459.
 14. Kang, M, Choung, S.J and Park, J.Y, photocatalytic degradation of methylene blue dye using fe2o3/tio2 core-shell (2003) *Catal. Today*, 87, 87.
 15. Wan, J, Li, H, and Chen, K, solid- state synthesis of the zno-fe3o4 nanocomposites; structural and magnetic properties (2009) *Mater. Chem. Phys.*, 114, 30.
 16. Yan, W, Fan, H and Yang, C, ultra fast synthesis and enhanced photocatalytic properties of alpha fe2o3/zno core-shell structure (2011) *Mater. Lett.*, 65, 1595.
 17. Ghows, N, Entezari, M.H,(2011) Exceptional Catalytic efficiency in mineralization of the reactive textile azo dye(RB5) by a combination of ultrasound and core-shell nanoparticles (CdS/TiO₂); *J. Hazar., Mat.*, 195, 132-138.
 18. Zhang, X, Xie, Y, Chen, H, Guo, J, Alan Meng, Li, C,(2014) One-dimensional mesoporous Fe₂O₃@TiO₂ core-shell nanocomposites: Rational design, synthesis and application as high-performance photocatalyst in visible and UV light region, *Appl., Surf., Sci.*, 317, 43-48.
 19. Jiang, W, Mo Zhang, Wang, J, Liu, Y, Yongfa, Z,(2014) Dramatic visible activity in phenol degradation of TCNQ@TiO₂ photocatalyst with core-shell structure, *Appl., Catal., B: Environ.*, 160-161 44-50.
 20. Mei Gui, M, Siang-Piao Chai, Bo-Qing Xu, Mohamed, A.R,(2014) Enhanced visible light responsive MWCNT/TiO₂ core-shell nanocomposites as the potential photocatalyst for reduction of CO₂ into methane, *Solar Energy Mater. Solar Cells*, 122, 183-189.
 21. Dong, W, Feng Pan, Xu, L, Zheng, M, Haur Sow, C, Kai Wu, Guo Qin Xu, W. Chen, W(2015), Facile synthesis of CdS@TiO₂ core-shell nanorods with controllable shell thickness and enhanced photocatalytic activity under visible light irradiation, *Appl., Surf. Sci.*, 349, 279-286.